Computers & Structures Vol. 40, No. 3, pp. 659–678, 1991
Printed in Great Britain.

0045-7949/91 $3.00 + 0.00
Pergamon Press plc

A COMPARATIVE STUDY OF C^0 AND C^1 ELEMENTS FOR LINEAR AND NONLINEAR TRANSIENT DYNAMICS OF BUILDING FRAMES

T. KANT and S. R. MARUR
Department of Civil Engineering, Indian Institute of Technology, Powai, Bombay 400 076, India

(*Received* 26 *April* 1990)

Abstract—The C^1 continuous element based on the Euler–Bernoulli theory of bending and the C^0 continuous element based on Timoshenko's theory of bending are compared for their computational efficiency and economy for the analysis of inelastic frames subjected to transient dynamic loads. Moreover, the size of a C^0 mesh (with only linear elements) is evaluated, which is computationally equivalent to C^1 Hermitian element. Also the ranges of slenderness ratio, in which both these elements are effective and the limits of aspect ratio below which they fail are also determined through the numerical studies.

1. INTRODUCTION

The well-known classic Euler–Bernoulli theory of bending, assumes the transverse plane section is normal to the reference middle plane before bending to remain so even during bending and neglects the transverse shear deformation totally. When this theory is formulated using the displacement based finite elements, the slope continuity between adjacent elements, becomes a must, known as C^1 continuity, as the bending rotation becomes equal to the first derivative of the transverse displacement. This theory thus requires the transverse displacement field to be C^1 continuous. This formulation has widely been in use [1–3] for the transient dynamic analysis of inelastic frames.

As the aspect ratio (length/depth) of the frame element becomes smaller, the transverse shear deformation becomes so predominant that it renders any analysis inaccurate unless and until it is accounted for in the basic formulation. The correction for transverse shear was first incorporated by Timoshenko [4] for the vibration problems. When finite elements were used to analyse deeper sections, using Timoshenko's theory, independent interpolation functions for slopes and displacements were used, making the displacements C^0 continuous. Many such elements have been reported [5–8] in the past.

Inspite of ease of formulation and development of computer code [5], the C^0 elements, however, have not been in use, particularly for the analysis of inelastic frames under transient loadings. An attempt is made here on the following lines:

(a) to use C^0 elements for transient dynamic analysis of inelastic and elastic frames and compare their computational efficiency and economy with C^1 elements,
(b) to find the size of C^0 mesh, consisting of linear elements, which must be comparable in performance to C^1 elements based on Hermitian cubic polynomial, and
(c) to ascertain the ranges of slenderness ratio in which C^0 and C^1 elements are effective in predicting the response and also the limits of these ratios, below which they fail.

2. SOLUTION OF DYNAMIC EQUILIBRIUM EQUATION

The governing equation of dynamic equilibrium, in the incremental form

$$[M]\{\Delta\ddot{d}\}_{n+1} + [C]\{\Delta\dot{d}\}_{n+1} + \{\Delta p\}_{n+1} = \{\Delta f\}_{n+1}, \tag{1}$$

where $[M]$ and $[C]$ are the mass and damping matrices; $\{\Delta p\}_{n+1}$ and $\{\Delta f\}_{n+1}$ are the incremental internal and external force vectors, respectively at $t = t_{n+1}$, is solved using the modified central difference predictor method [9], to obtain the displacements, velocities, and accelerations at every time step.

3. EULER–BERNOULLI THEORY WITH C^1 FORMULATION

3.1. *Displacement field and strain displacement relationship*

The displacement field $U(x, y)$, $V(x, y)$ of a frame member can be expressed in terms of middle plane axial displacement $u(x)$, transverse displacement $v(x)$ and the rotation of the normal about z axis $\theta_z(x)$ as

$$U(x, y) = u(x) - y\theta_z(x), \tag{2}$$

$$V(x, y) = v(x), \tag{3}$$

$$\theta_z(x) = \frac{\partial v(x)}{\partial x}. \tag{4}$$

The strain at any point (x, y) is given by

$$\epsilon(x, y) = \frac{\partial U(x, y)}{\partial x} \tag{5}$$

which becomes after the substitution of eqn (2)

$$\epsilon(x, y) = \frac{\partial u(x)}{\partial x} - y\frac{\partial \theta_z(x)}{\partial x} = \epsilon^a + \epsilon^b(x, y). \tag{6}$$

Using the standard finite element representation [10], the axial strain can be expressed as

$$\epsilon^a = \begin{bmatrix} -1 & 1 \\ L & L \end{bmatrix} \begin{Bmatrix} u_i \\ u_j \end{Bmatrix} = \{B_a\}^T \{d_a^e\}, \tag{7}$$

where u_i and u_j are the axial displacements of nodes i and j of a frame element and $\{d_a^e\}$ is the axial displacement vector of the element.

Similarly the bending component of axial strain can be expressed with the use of cubic Hermitian polynomial as

$$\epsilon^b(\xi, \eta) = \frac{d}{2}\eta \begin{bmatrix} \frac{-6\xi}{L^2} & \frac{(1-3\xi)}{L} & \frac{6\xi}{L^2} & \frac{(1+3\xi)}{L} \end{bmatrix} \times \begin{Bmatrix} v_i \\ \theta_i \\ v_j \\ \theta_j \end{Bmatrix} = \{B_b(\xi, \eta)\}^T \{d_b^e\}, \tag{8}$$

where d is the depth of the cross-section and $\{d_b^e\}$ is the vector of bending displacements of the element.

The strain at any generic point (ξ, η) at $t = t_{n+1}$ can be expressed as

$$\epsilon(\xi, \eta)_{n+1} = \epsilon^a_{n+1} + \epsilon^b(\xi, \eta)_{n+1} \tag{9}$$

and the incremental strain due to the incremental displacement vector $\{\Delta d^e\}_{n+1}$ as

$$\Delta\epsilon(\xi, \eta)_{n+1} = \{B_a\}^T \{\Delta d_a^e\}_{n+1} + \{B_b(\xi, \eta)\}^T \{\Delta d_b^e\}_{n+1} = \Delta\epsilon^a_{n+1} + \Delta\epsilon^b(\xi, \eta)_{n+1}. \tag{10}$$

3.2. *Plastification of cross-section*

The stresses are evaluated at the Gauss points across the depth of the cross-section. Whenever a Gauss point reaches the yield stress, that point alone is considered to have become plastic, while other points continue to remain in their respective states of stress. As the strain increases, due to the increased displacements, the extreme Gauss points attain the yield stress first and with the further increase in the strain, the interior Gauss points also reach the yield stress. When all the Gauss points reach the yield stress, the cross section can be said to have become completely plastic.

3.3. *Stress–strain relationship*

The incremental elastic stress corresponding to the incremental strain can be given by

$$\Delta\sigma(\xi, \eta)^{el}_{n+1} = E\,\Delta\epsilon(\xi, \eta)_{n+1}, \tag{11}$$

where E is the Young's modulus of the material. When the material becomes plastic, the total stress at $t = t_{n+1}$, evaluated based on elastic incremental stress is given as

$$\sigma(\xi, \eta)^{el}_{n+1} = \Delta\sigma(\xi, \eta)^{el}_{n+1} + \sigma(\xi, \eta)_n, \tag{12}$$

where $\sigma(\xi, \eta)_n$ is the known stress at that point at $t = t_n$ and the superscript el in $\sigma(\xi, \eta)^{el}_{n+1}$ denotes that, this total stress is based on an assumed elastic behaviour of the material between $t = t_n$ and $t = t_{n+1}$.

But during the same time interval, the material could either have remained elastic or gone plastic or become elastic again during unloading or reloading phases. So $\sigma(\xi, \eta)^{el}_{n+1}$ is to be corrected so as to make it represent the actual state of stress of the material at that time interval, using the stress–strain diagram of the material [11].

If the corrected stress can be represented as $\sigma(\xi, \eta)^c_{n+1}$, where the superscript c stands for the corrected quantity, then the incremental corrected stress at $t = t_{n+1}$, can be expressed as

$$\Delta\sigma(\xi, \eta)^c_{n+1} = \sigma(\xi, \eta)^c_{n+1} - \sigma(\xi, \eta)_n. \tag{13}$$

3.4. *Internal resisting force vector*

The incremental axial internal resisting force vector can be given as

$$\{\Delta p_a\}_{n+1} = \int_{V_e} \{B_a\}^T \Delta\sigma(\xi, \eta)^c_{n+1}\, dv, \tag{14}$$

which on expansion becomes

$$\{\Delta p_a\}_{n+1} = \frac{L}{2}\int_{-1}^{1} \left[\frac{bd}{2}\int_{-1}^{1} \{B_a\}^T \times \Delta\sigma(\xi, \eta)^c_{n+1}\, d\eta\right] d\xi, \tag{15}$$

where b is the breadth and L is the length of the member.

The incremental bending internal resisting force vector can be given by

$$\{\Delta p_b\}_{n+1} = \int_{V_e} \{B_b(\xi, \eta)\}^T \Delta\sigma(\xi, \eta)^c_{n+1}\, dv \tag{16}$$

which can be expanded as

$$\{\Delta p_b\}_{n+1} = \frac{L}{2}\int_{-1}^{1} \left[\frac{bd}{2}\int_{-1}^{1} \{B_b(\xi, \eta)\}^T \times \Delta\sigma(\xi, \eta)^c_{n+1}\, d\eta\right] d\xi. \tag{17}$$

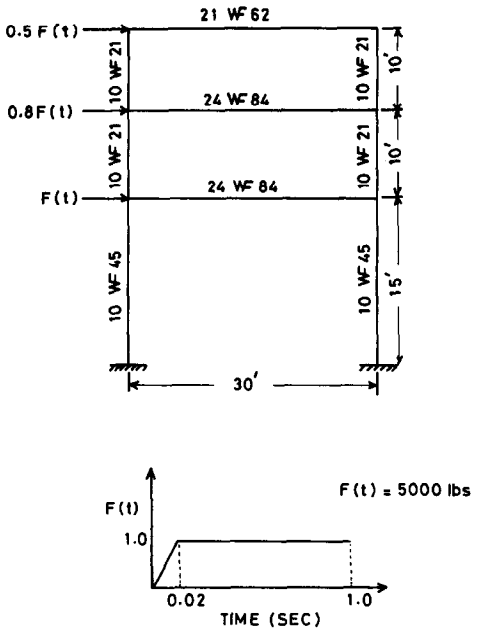

Fig. 1. Three storey frame, subjected to concentrated transient loads [17].

When the vectors $\{\Delta p_a\}_{n+1}$ and $\{\Delta p_b\}_{n+1}$ are appropriately assembled, the incremental internal resisting force vector $\{\Delta p^e\}_{n+1}$ is obtained. While employing Gaussian quadrature, to carry out the numerical integration to evaluate $\{\Delta p^e\}$ at all time steps, three span wise Gauss points and three depth wise Gauss stations are employed.

3.5. *Mass and damping matrices*

The mass is assumed to be lumped at nodal coordinates, where the translational degrees of freedom are defined and the inertial effect associated with the rotational degree of freedom is evaluated by calculating the mass moment of inertia of the fraction of the frame segment about the nodal points. The lumped mass matrix for a frame member can be given by

$$[M^e] = \begin{bmatrix} \frac{\bar{m}L}{2} & & & & & \\ & \frac{\bar{m}L}{2} & & & & \\ & & \frac{\bar{m}L^3}{24} & & & \\ & & & \frac{\bar{m}L}{2} & & \\ & & & & \frac{\bar{m}L}{2} & \\ & & & & & \frac{\bar{m}L^3}{24} \end{bmatrix}, \tag{18}$$

where $\bar{m}$ is the mass per unit length of the frame member. When Rayleigh's damping is adopted along with the central difference operators, the damping matrix can be given [12] as

$$[C^e] = \alpha[M^e] \tag{19a}$$

where α is a constant given by

$$\alpha = 2\xi_r\omega_r \tag{19b}$$

where ξ_r and ω_r are the damping factor and circular frequency for the rth mode.

3.6. *Critical time step*

The stability analysis of central difference schemes restricts the time step length [13] to

$$(\Delta t) \leqslant (\Delta t)_{cr} = \frac{2}{\omega_{\max}}, \tag{20}$$

where $\omega_{\max}$ is the highest circular frequency of the finite element mesh. As the highest system eigenvalue is always less than the highest element eigenvalue [14], using the highest element eigenvalue in eqn (20) will be an error on the safer side. Moreover, the free vibration analysis of the system need not be carried out, only to evaluate $(\Delta t)_{cr}$.

Belytschko [15] evaluated the element frequency from the product of stiffness and inverse of mass matrices as the natural frequency of a freely vibrating system is given as

$$\omega^2 = \frac{k}{m}. \tag{21}$$

For axial displacement, the product of stiffness and inverse of mass matrix is given by

$$[K_a][M_a]^{-1} = \frac{2AE}{\bar{m}L^2}\begin{bmatrix} 1 & -1 \\ -1 & 1 \end{bmatrix}. \tag{22}$$

The highest frequency of the element, for axial displacements is given from eqn (22) as

$$\omega_a^2 = \frac{4AE}{\bar{m}L^2} = \frac{4c^2}{L^2}, \tag{23}$$

where $c^2 = E/\rho$, where c is the wave speed in the element and ρ is the mass density.

Similarly the diagonal elements of $[K_b][M_b]^{-1}$ is given as

$$\begin{bmatrix} \frac{24EI}{\bar{m}L^4} & & & \\ & \frac{96EI}{\bar{m}L^4} & & \\ & & \frac{24EI}{\bar{m}L^4} & \\ & & & \frac{96EI}{\bar{m}L^4} \end{bmatrix} \tag{24}$$

Table 1. Comparison of displacements of the frame with flexible girders

Maximum displacement of	Response by C^1 elements (inches)	Response by Biggs [17] (inches)
First storey	0.799	0.776
Second storey	1.193	1.145
Third storey	1.348	1.300

and the highest frequency corresponding to flexural displacements is given from the matrix given by eqn (24) as

$$\omega_b^2 = \frac{192EI}{\bar{m}L^4} = \left[\frac{192c^2r_g^2}{L^4}\right] \tag{25}$$

where the radius of gyration of the cross-section $r_g = I/A$ and $c^2 = E/\rho$.

The higher value of the two, given by the eqns (23) and (25) is used in eqn. (20) to evaluate $(\Delta t)_{cr}$ for C^1 continuous elements.

4. TIMOSHENKO'S THEORY WITH C^0 FORMULATION

4.1. *Layered concept and plastification of cross-section*

In this formulation, the cross-section is split into a number of layers and the layer midpoint stress is assumed to represent the state of stress of the entire layer itself. Whenever the midpoint stress of a layer reaches the yield value, that layer alone is assumed to have become plastic, while the rest of the layers continue to remain in their respective states of stress. With the increase in strain, the stresses at the midpoints of outer most layers reach the value of yield stress first and gradually the stresses at the midpoints of interior layers also attain the yield value. When all the layers reach the yield stress, the section is said to have become plastic. The gradual plastification of the cross-section is modelled more realistically by this concept and with the increase in the number of layers, modelling of plastification becomes very close to the reality.

4.2. *Displacement field and strain displacement relationship*

The axial and transverse displacements are expressed as given by eqns (2) and (3), and the rotation of the cross-section inclusive of that due to transverse shear deformation can be expressed as

$$\theta_z(x) = \frac{\partial v(x)}{\partial x} + \phi, \tag{26}$$

where ϕ is the rotation due to transverse shear deformation.

Using the two noded, linear [5–7] element, the displacements can be expressed as

$$u = \sum_{i=1}^{2} N_i u_i, \tag{27a}$$

$$v = \sum_{i=1}^{2} N_i v_i, \tag{27b}$$

$$\theta = \sum_{i=1}^{2} N_i \theta_i, \tag{27c}$$

where

$$N_1 = \frac{(1-\xi)}{2}, \tag{28a}$$

and

$$N_2 = \frac{(1+\xi)}{2}. \tag{28b}$$

The axial component of axial strain is given as

$$\epsilon_a = \begin{bmatrix} \frac{\partial N_1}{\partial x} & \frac{\partial N_2}{\partial x} \end{bmatrix} \begin{Bmatrix} u_1 \\ u_2 \end{Bmatrix} = \{B_a\}^T \{d_a^e\}. \tag{29}$$

Any generic point in the frame can be denoted by $(\xi, \bar{y})$, where ξ is a Gauss point along the length of the member and $\bar{y}$ is the distance between the midpoint of a layer and the neutral axis of the cross-section. The bending component of axial strain at $(\xi, \bar{y})$ is given by

$$\epsilon_b(\xi, y) = -\bar{y} \sum_{i=1}^{2} \frac{\partial N_i}{\partial x} \theta_i \tag{30}$$

which when expressed in matrix notation becomes as

$$\epsilon_b(\xi, \bar{y}) = -\bar{y} \begin{bmatrix} \frac{\partial N_1}{\partial x} & \frac{\partial N_2}{\partial x} \end{bmatrix} \begin{Bmatrix} \theta_1 \\ \theta_2 \end{Bmatrix} = \{B_b(\xi, \bar{y})\}^T \{d_b^e\}. \tag{31}$$

Table 2. Comparison of displacements of the frame with rigid girders

Maximum displacement of	Response by C^1 elements (inches)	Response by Biggs [17] (inches)
First storey	0.691	0.697
Second storey	0.981	0.988
Third storey	1.087	1.130

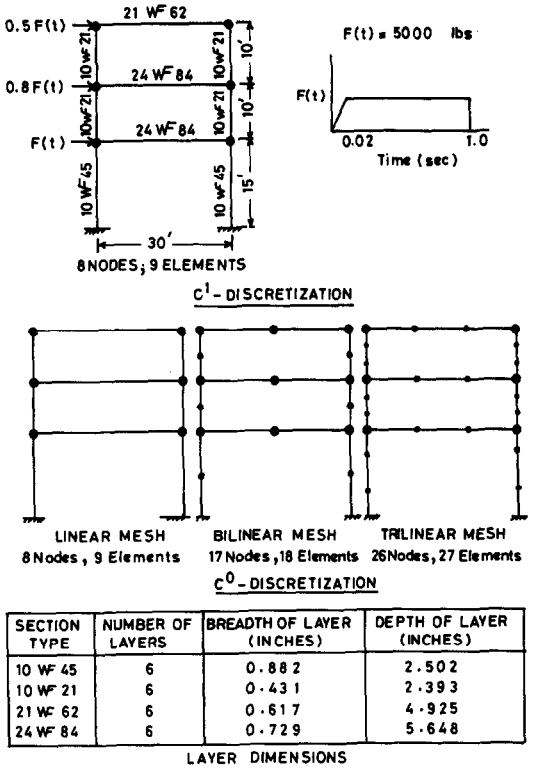

SECTION TYPE	NUMBER OF LAYERS	BREADTH OF LAYER (INCHES)	DEPTH OF LAYER (INCHES)
10 WF 45	6	0.882	2.502
10 WF 21	6	0.431	2.393
21 WF 62	6	0.617	4.925
24 WF 84	6	0.729	5.648

LAYER DIMENSIONS

Fig. 2. C^0 discretization of three storey frame [17].

The shear strain can be expressed as

$$\gamma_{\xi\eta} = -\sum_{i=1}^{2} N_i\theta_i + \sum_{i=1}^{2} \frac{\partial N_i}{\partial x} v_i \tag{32}$$

and expressed in matrix form as

$$\gamma_{\xi\eta} = \left[\frac{\partial N_1}{\partial x} - N_1 \frac{\partial N_2}{\partial x} - N_2\right] \begin{Bmatrix} v_1 \\ \theta_1 \\ v_2 \\ \theta_2 \end{Bmatrix} = \{B_s(\xi)\}^T \{d_s^e\}. \tag{33}$$

The incremental axial and shear strains at $t = t_{n+1}$ can be expressed as

$$\Delta\epsilon(\xi, \bar{y})_{n+1} = \{B_a\}^T \{\Delta d_a^e\}_{n+1} + \{B_b(\xi, \bar{y})\}^T \{\Delta d_b^e\}_{n+1} \tag{34}$$

and

$$\Delta\gamma(\xi)_{n+1} = \{B_s(\xi)\}^T \{\Delta d_s^e\}_{n+1}. \tag{35}$$

4.3. *Stress–strain relationship*

The incremental elastic stress of a layer is given by

$$\Delta\sigma(\xi, \bar{y})_{n+1}^{el} = E_l \Delta\epsilon(\xi, \bar{y})_{n+1}, \tag{36}$$

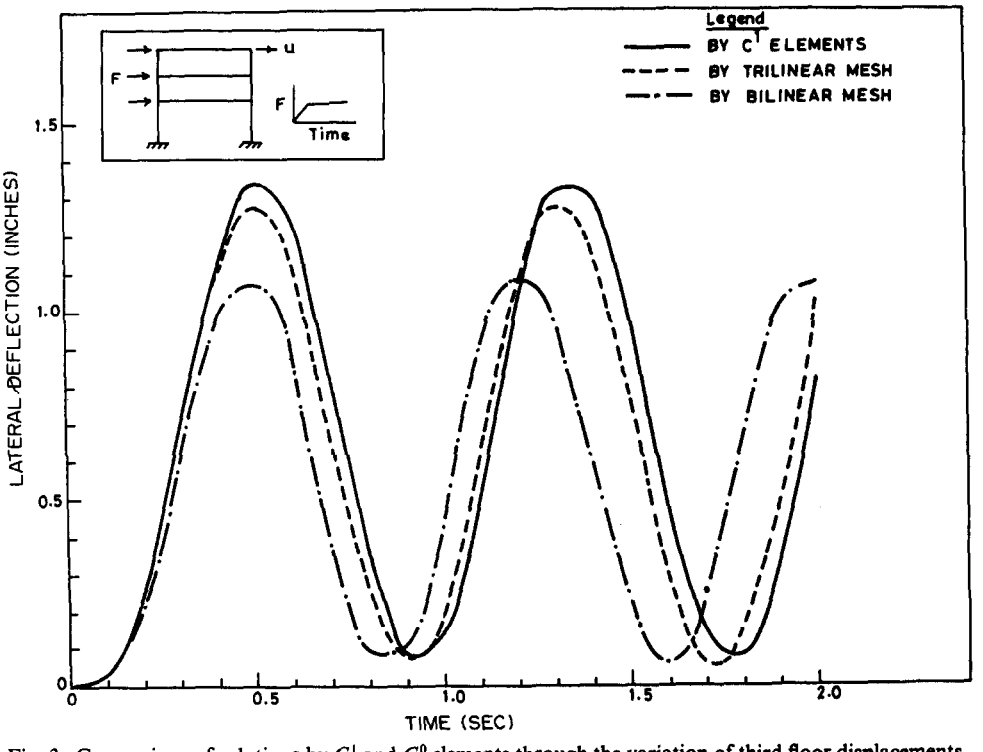

Fig. 3. Comparison of solutions by C^1 and C^0 elements through the variation of third floor displacements with time [17].

Table 3. Comparison of computational costs of C^1 and C^0 meshes (example 1)

Mesh type	(Δt) adopted (sec)	Range of integration (sec)	Number of steps	CPU time (sec)
C^1	0.1E − 3	2.0	2E4	286
Linear	0.1E − 3	2.0	2E4	380
Bilinear	0.5E − 4	2.0	4E4	1512
Trilinear	0.25E − 4	2.0	8E4	5922

where E_l is the Young's modulus of the layer. When materially nonlinear analysis is to be carried out, the total elastic stress at $t = t_{n+1}$ is given by

$$\sigma(\xi, \bar{y})^{el}_{n+1} = \Delta\sigma(\xi, \bar{y})^{el}_{n+1} + \sigma(\xi, \bar{y})_n, \tag{37}$$

where $\sigma(\xi, \bar{y})_n$ is the corrected layer stress at $t = t_n$. The stress $\sigma(\xi, \bar{y})^{el}_{n+1}$ is to be corrected according to the material stress strain curve to make it represent the actual material stress. The corrected incremental stress is then given as

$$\Delta\sigma(\xi, \bar{y})^{c}_{n+1} = \sigma(\xi, \bar{y})^{c}_{n+1} - \sigma(\xi, \bar{y})_n. \tag{38}$$

The incremental shear stress is evaluated as

$$\Delta\tau(\xi)^{l}_{n+1} = G_l \Delta\gamma(\xi)_{n+1}, \tag{39}$$

where $\Delta\tau(\xi)^{l}_{n+1}$ is the shear stress of a layer and G_l is the layer shear modulus.

4.4. *Internal resisting force vector*

The incremental axial force vector can be expressed as

$$\{\Delta p_a\}_{n+1} = \int_0^L \int_{-d/2}^{d/2} \int_b \{B_a\}^T \times \Delta\sigma(\xi, \bar{y})^{c}_{n+1}\, dz\, dy\, dx \tag{40}$$

and by applying the layer concept it becomes

$$\{\Delta p_a\}_{n+1} = \int_{-1}^{1} \{B_a\}^T \times \left[\sum_{l=1}^{TNL} b_l t_l \Delta\sigma(\xi, \bar{y})^{c}_{n+1}\right] |J|\, d\xi, \tag{41}$$

where TNL stands for total number of layers in the cross-section, and $|J|$ for the determinant of the Jacobian.

The incremental bending force vector is given by

$$\{\Delta p_b\}_{n+1} = \int_0^L \int_{-d/2}^{d/2} \int_b \{B_b(\xi, \bar{y})\}^T \times \Delta\sigma(\xi, \bar{y})^{c}_{n+1}\, dz\, dy\, dx \tag{42}$$

and after applying the layer concept

$$\{\Delta p_b\}_{n+1} = \int_{-1}^{1} \{B_b(\xi)\}^T \times \left[\sum_{l=1}^{TNL} b_l t_l \bar{y}\, \Delta\sigma(\xi, \bar{y})^{c}_{n+1}\right] |J|\, d\xi \tag{43a}$$

where

$$\{B_b(\xi)\}^T = -\begin{bmatrix} \dfrac{\partial N_1}{\partial x} & \dfrac{\partial N_2}{\partial x} \end{bmatrix}. \tag{43b}$$

Incremental shear force is given by

$$\{\Delta p_s\}_{n+1} = \int_0^L \int_{-d/2}^{d/2} \int_b \{B_s(\xi)\}^T \times \Delta\tau(\xi)^{l}_{n+1}\, dz\, dy\, dx \tag{44}$$

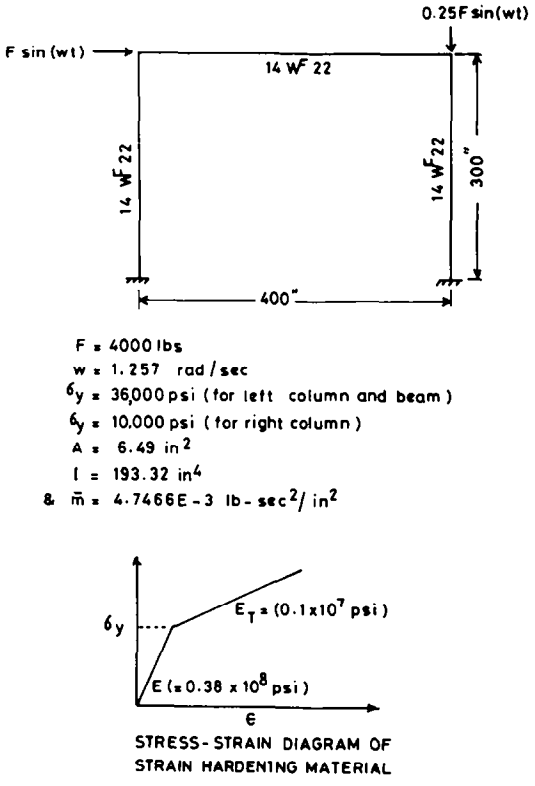

Fig. 4. Frame subjected to sinusoidal load [18].

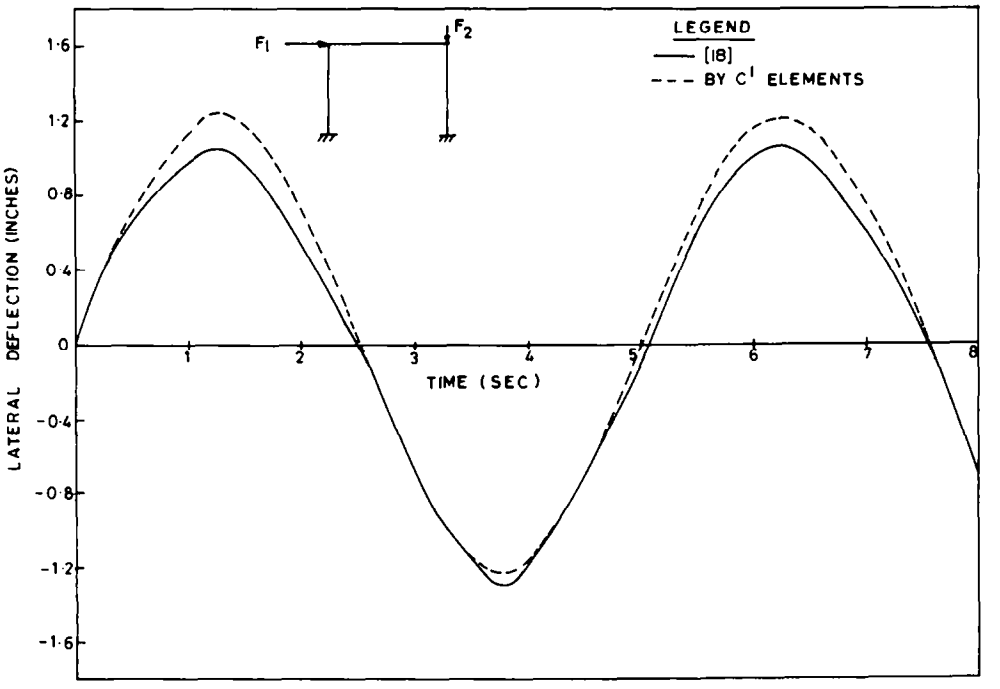

Fig. 5. Time history of elastic horizontal displacement of top right node of the frame.

$$\{\Delta p_s\}_{n+1} = \int_{-1}^{1} \{B_s(\xi)\}^T \times \left[\sum_{l=1}^{TNL} b_l t_l \Delta\tau(\xi)'_{n+1}\right] |J| \, d\xi. \quad (45)$$

While evaluating the shear forces, the shear rigidity GA is replaced by $G\hat{A}$, where the area $\hat{A}$ is given by A/ν. The parameter ν is a correction factor to allow for cross-sectional warping, which is taken to be 1.2 for rectangular sections. Moreover, $\{\Delta p_s\}$ is evaluated using reduced integration to cure the shear locking, when slender members are analysed. When the vectors $\{\Delta p_a\}$, $\{\Delta p_b\}$ and $\{\Delta p_s\}$ are appropriately assembled, the internal resisting force vector is obtained.

4.5. *Specially lumped mass matrix*

The simultaneous use of central difference operators and the C^0 formulation, requires the consistent mass matrix to be converted into a diagonal one. The procedure to achieve this objective, known as 'special lumping' outlined by Hinton *et al.* [16] is adopted here for the linear element.

The consistent mass matrix can be expressed as

$$[M^e] = \int_0^L [N^e]^T [m^e] [N^e] \, dv \quad (46a)$$

in which

$$[m^e] = \begin{bmatrix} \rho bd & & \\ & \rho bd & \\ & & \dfrac{\rho bd^3}{12} \end{bmatrix} \quad (46b)$$

and $[N^e]$ is the matrix of shape functions of an element. The consistent mass matrix for the element is given by

$$[M^e] = \begin{bmatrix} \dfrac{\bar{m}L}{3} & & & \dfrac{\bar{m}L}{6} & & \\ & \dfrac{\bar{m}L}{3} & & & \dfrac{\bar{m}L}{6} & \\ & & \dfrac{\bar{m}Ld^2}{36} & & & \dfrac{\bar{m}Ld^2}{72} \\ \dfrac{\bar{m}L}{6} & & & \dfrac{\bar{m}L}{3} & & \\ & \dfrac{\bar{m}L}{6} & & & \dfrac{\bar{m}L}{3} & \\ & & \dfrac{\bar{m}Ld^2}{72} & & & \dfrac{\bar{m}Ld^2}{36} \end{bmatrix} \quad (47)$$

A scaling factor, defined as the ratio of the total mass of the element to the sum of the masses (in the diagonal elements) corresponding to any one translational degree of freedom, is calculated as

$$\text{scaling factor} = (\bar{m}L) \Big/ \left(\frac{2\bar{m}L}{3}\right) = \frac{3}{2}. \quad (48)$$

When all the diagonal elements are scaled by this factor and the off-diagonal elements are made equal

to zero, the specially lumped mass matrix is obtained as

$$[M^c] = \begin{bmatrix} \frac{\bar{m}L}{2} & & & & & \\ & \frac{\bar{m}L}{2} & & & & \\ & & \frac{\bar{m}Ld^2}{24} & & & \\ & & & \frac{\bar{m}L}{2} & & \\ & & & & \frac{\bar{m}L}{2} & \\ & & & & & \frac{\bar{m}Ld^2}{24} \end{bmatrix}. \quad (49)$$

and the damping matrix is expressed as in C^1 formulation as

$$[C^c] = \alpha[M^c]. \quad (50)$$

4.6. *Critical time step*

Expressions for evaluating $(\Delta t)_{cr}$ for C^0 elements, following Belytschko's expressions for C^1 elements are derived. For axial displacements, the frequency for C^0 elements is the same as that of C^1 elements [as given by eqn (23)].

The stiffness matrix for the linear element using reduced integration for shear terms is given by

$$[K_b] = \begin{bmatrix} \frac{G\hat{A}}{L} & \frac{G\hat{A}}{2} & -\frac{G\hat{A}}{L} & \frac{G\hat{A}}{2} \\ & \left[\frac{EI}{L} + \frac{G\hat{A}L}{4}\right] & -\frac{G\hat{A}}{2} & \left[\frac{-EI}{L} + \frac{G\hat{A}L}{4}\right] \\ & & \frac{G\hat{A}}{L} & -\frac{G\hat{A}}{2} \\ & & -\frac{G\hat{A}}{2} & \left[\frac{EI}{L} + \frac{G\hat{A}L}{4}\right] \end{bmatrix} \quad (51)$$

and the diagonal elements of $[K_b][M_b]^{-1}$ are given by

$$\begin{bmatrix} \frac{G\hat{A}}{L}\frac{2}{\bar{m}L} & & & \\ & \left[\frac{EI}{L} + \frac{G\hat{A}L}{4}\right]\frac{24}{\bar{m}Ld^2} & & \\ & & \frac{G\hat{A}}{L}\frac{2}{\bar{m}L} & \\ & & & \left[\frac{EI}{L} + \frac{G\hat{A}L}{4}\right]\frac{24}{\bar{m}Ld^2} \end{bmatrix} \quad (52)$$

and the frequency corresponding to flexural displacement is given by

$$\omega_b^2 = \frac{48}{\bar{m}Ld^2}\left[\frac{EI}{L} + \frac{G\hat{A}L}{4}\right] = \left[\frac{48c^2r_g^2}{L^2d^2} + \frac{12G\hat{A}}{\bar{m}d^2}\right]. \quad (53)$$

The higher one of the two given by eqns (23) and (53) is to be used in the condition (20) to evaluate the critical time step.

5. NUMERICAL EXAMPLES

The examples are chosen such that both C^0 and C^1 elements are used for frames with slender members in both elastic and inelastic conditions and in deep beams under going elastic and plastic deformations. All the computations were carried out on CYBER 180/840 computer in SINGLE PRECISION with 16 significant digits as word-length.

5.1. *C^0 mesh formation*

Every frame element, discretized by a C^1 element is also discretized by THREE C^0 elements, denoted as TRILINEAR MESH, by TWO C^0 elements represented as BILINEAR MESH and a C^0 element known as LINEAR MESH. The objective of such a discretization is to obtain meshes equivalent to quadratic and cubic elements with simple linear elements, as more number of lower order elements are computationally economical than few higher order elements. These discretizations form the basic ground for comparison of results of one mesh with another, with C^1 results and with those available in the literature.

5.2. *Examples*

Example 1. Biggs [17] has analysed a three storeyed frame with nodal dynamic loads as shown in Fig. 1 using modal superposition method. The same frame is analysed using C^1 elements, first with rigid girders and then with flexible girders.

Table 1 gives the displacements of flexible girders while Table 2 displays the maximum displacements of rigid girders. In both the cases, the close agreement between the results by C^1 elements and Biggs can be observed.

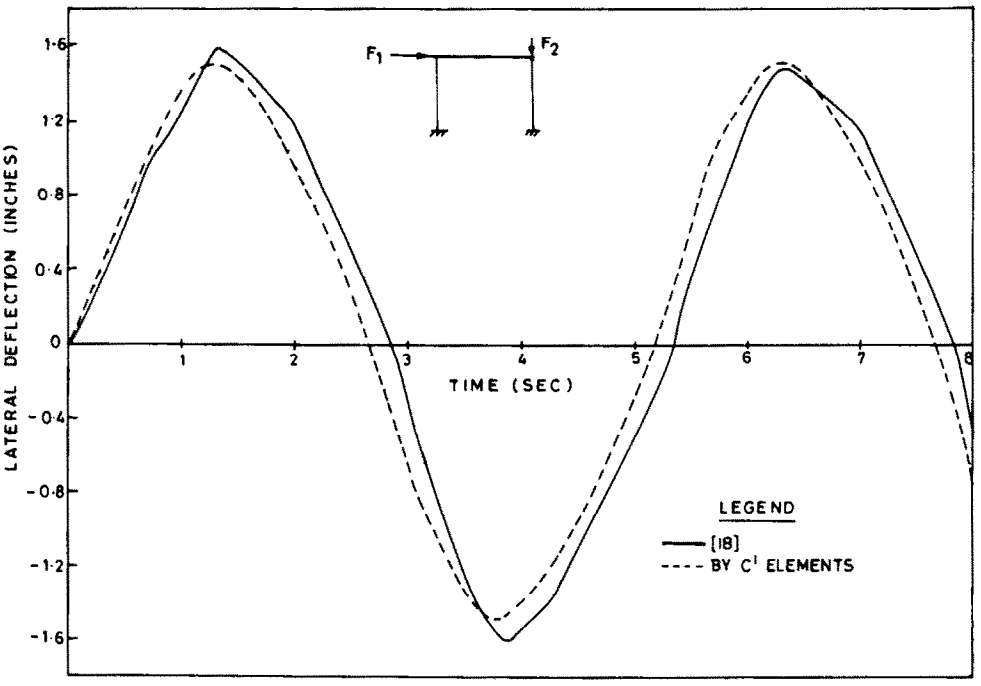

Fig. 6. Time history of elastoplastic strain hardening horizontal displacement of top right node of the frame.

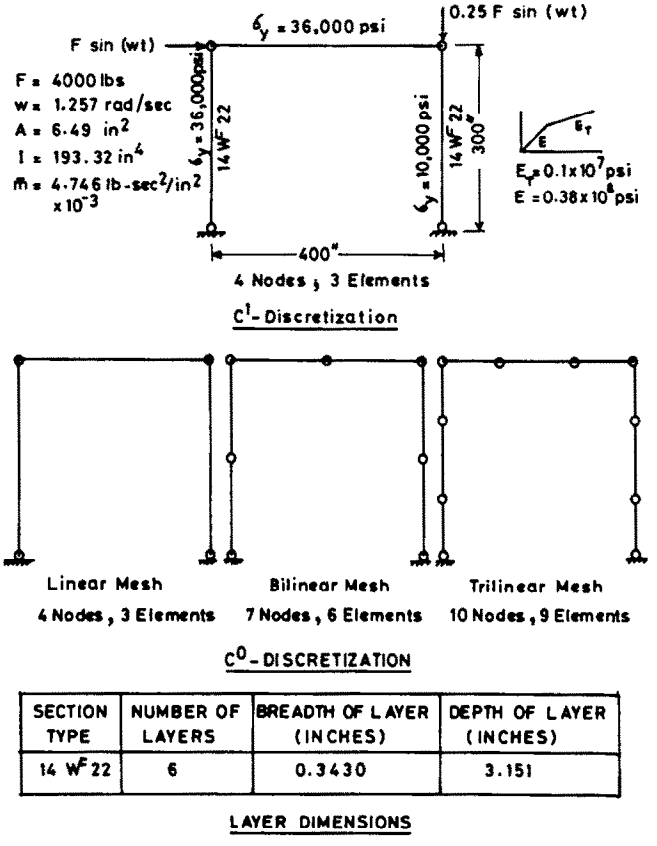

SECTION TYPE	NUMBER OF LAYERS	BREADTH OF LAYER (INCHES)	DEPTH OF LAYER (INCHES)
14 WF 22	6	0.3430	3.151

LAYER DIMENSIONS

Fig. 7. C^0 discretization of a sinusoidally loaded frame [18].

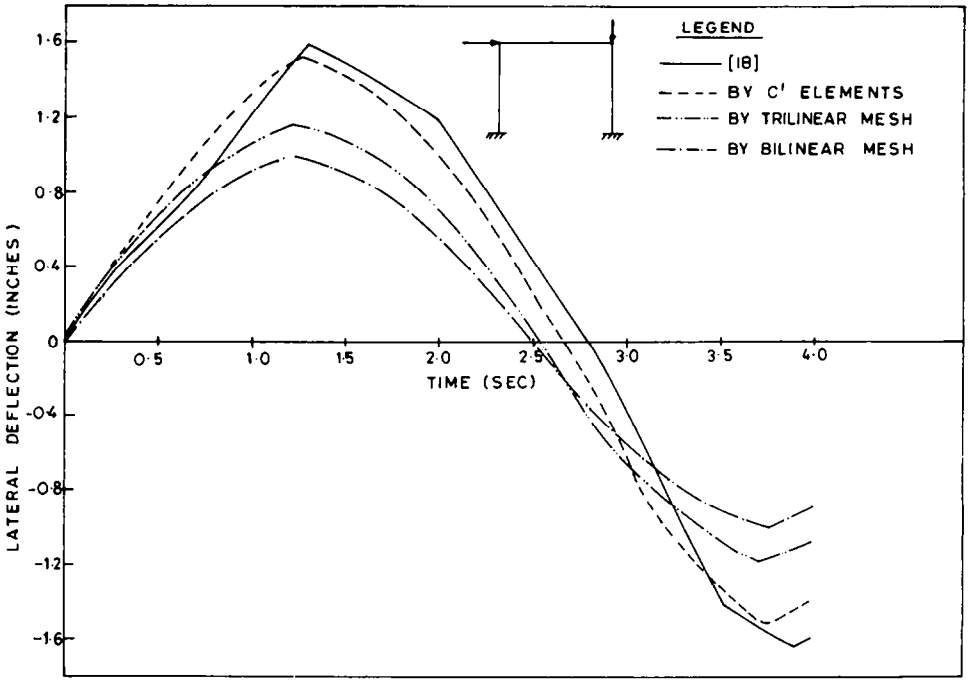

Fig. 8. Comparison of C^0 and C^1 elements through the horizontal (strain hardening) displacements of top right node of the frame.

Table 4. Comparison of computational costs of C^1 and C^0 meshes (example 2)

Mesh type	(Δt) adopted (sec)	Range of integration (sec)	Number of steps	CPU time (sec)
C^1	0.1E − 2	4.0	4E3	32
Linear	0.1E − 4	4.0	4E5	3200
Bilinear	0.1E − 4	4.0	4E5	6000
Trilinear	0.1E − 4	4.0	4E5	8800

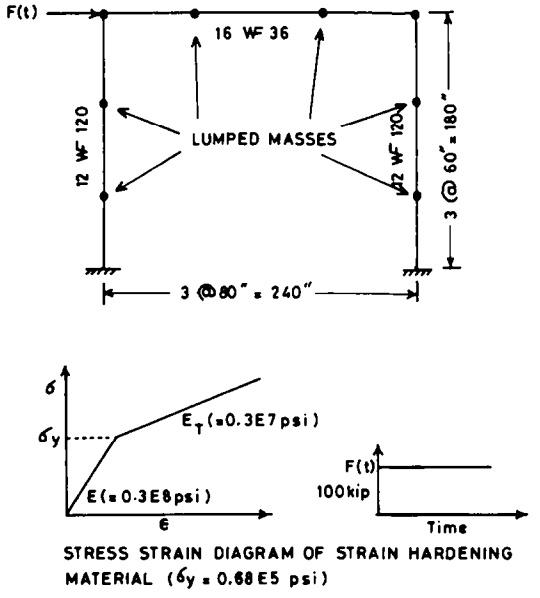

Fig. 9. Rectangular frame with lateral load and strain hardening material model [1].

While using C^0 elements, all the cross-sections are split into six layers and all the three types of meshes are adopted as shown in Fig. 2. The response history by trilinear and bilinear meshes along with that produced by C^1 are shown in Fig. 3.

The response by linear mesh was too small to be plotted in the same graph, as the first order polynomial shape functions are not adequate enough to predict the actual response. The trilinear mesh produces results very close to that of C^1 and bilinear results are slightly stiffer.

The computational costs are presented in Table 3 and it can be observed that C^0 meshes are comparatively time consuming.

Example 2. Hilmy and Abel [18] had considered a single storey portal frame as shown in Fig. 4 and is discretized by four C^1 elements. The elastic and elastoplastic responses are obtained and the displacement histories are plotted in Figs 5 and 6 which depict the agreement of C^1 results with the reference outputs.

While adopting C^0 meshes as shown in Fig. 7, the cross-section is split into six layers. The nonlinear

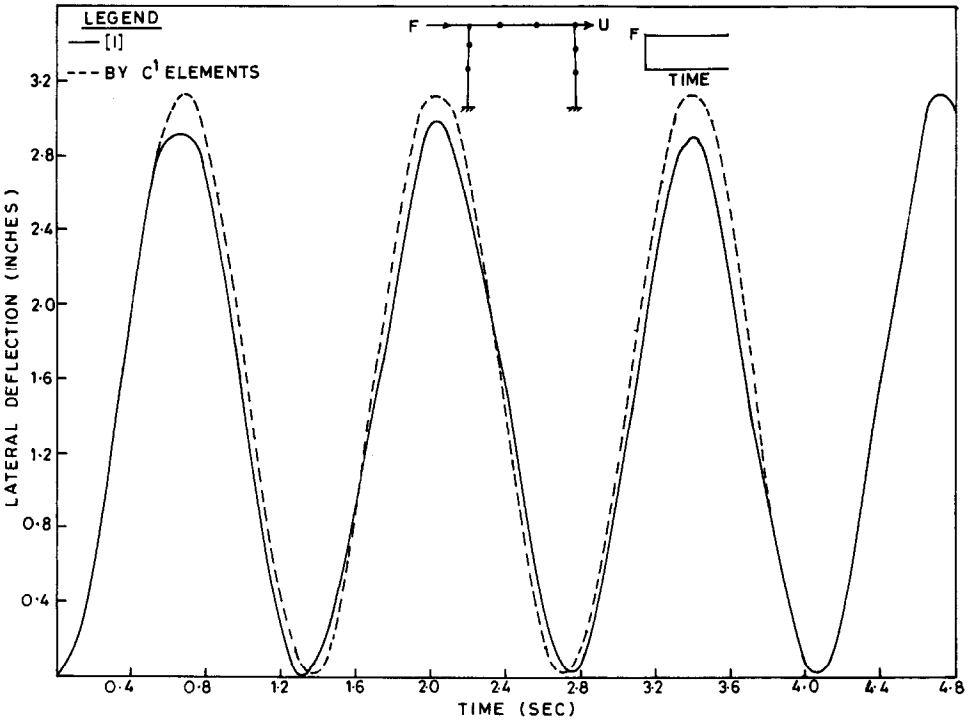

Fig. 10. Time history of elastic deflection of point of application of load.

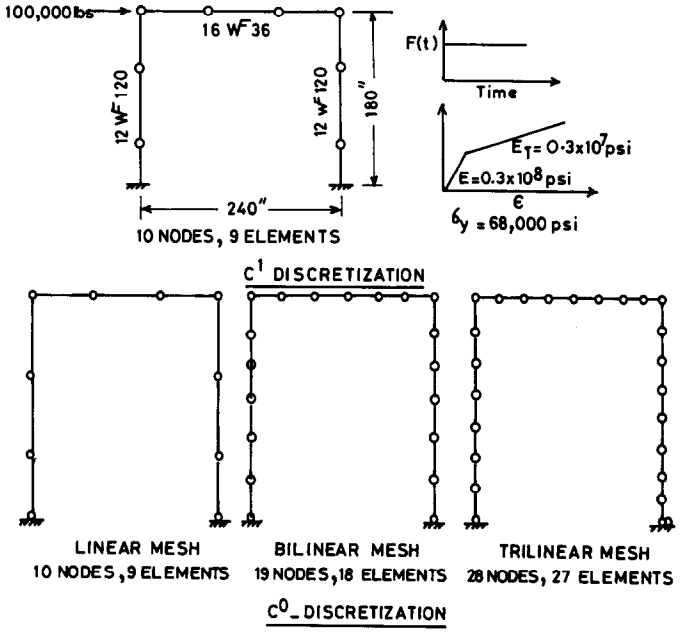

SECTION TYPE	NUMBER OF LAYERS	BREADTH OF LAYER (INCHES)	DEPTH OF LAYER (INCHES)
16 WF 36	6	0.4746	3.722
12 WF 120	6	1.858	3.167

LAYER DIMENSIONS

Fig. 11. C^0 discretization of a frame with suddenly applied load [1].

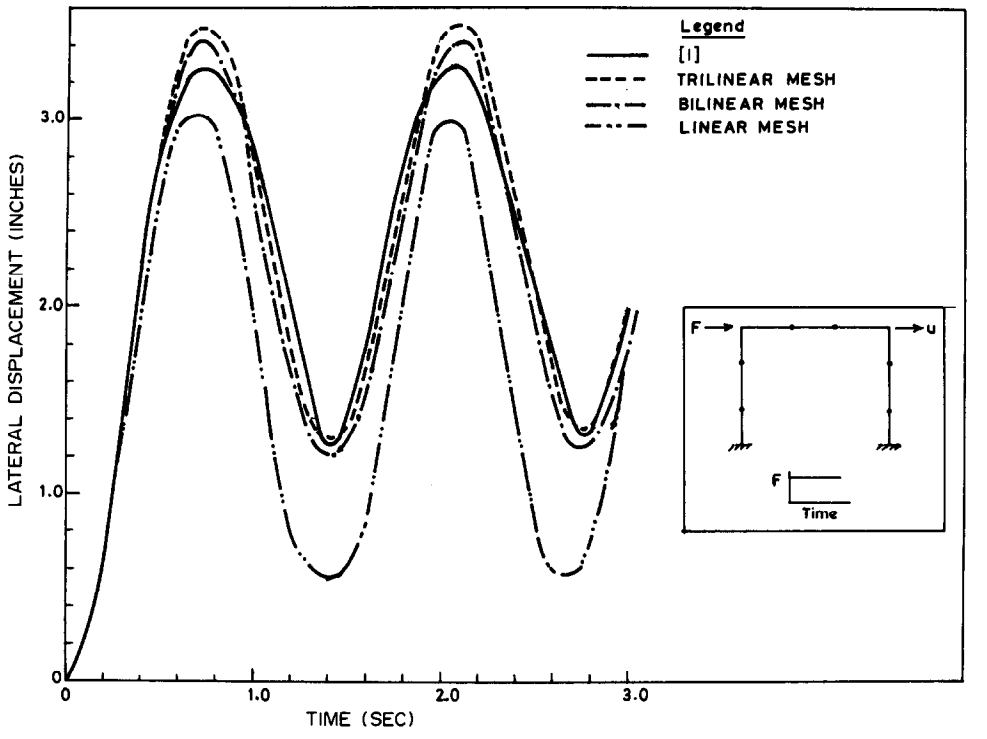

Fig. 12. Comparison of solutions by C^0 and C^1 elements through the variation of horizontal displacements with time.

response histories are given in Fig. 8 and the computational costs are shown in Table 4. The results by trilinear mesh are closer to C^1 but slightly stiffer. Bilinear mesh results are still stiffer while those by linear mesh are very small to be plotted. Computationally C^1 elements are economical.

Example 3. Toridis and Khozeimeh [1] had studied a single storeyed frame with the masses lumped at eight points as shown in Fig. 9. The actual lumped masses are multiplied by a factor of 625 to make the fundamental frequency of the frame very close to that of actual buildings. The frame has been discretized with nine C^1 elements, keeping the lumped mass positions of the reference frame as the nodes, for the elements. The elastic response is shown in Fig. 10 along with reference response.

The use of C^0 meshes with the layered cross-section are shown in Fig. 11 while the response history is in Fig. 12 along with the computational costs in Table 5.

In this particular example, as the number of elements are comparatively very high, (nine for linear mesh, eighteen for bilinear mesh and twenty seven for trilinear mesh) all the meshes produce results, which closely follow the displacement pattern of the reference output. Of all the three, trilinear mesh is very close to the reference curve while other two meshes yield slightly stiffer response histories. Here also the C^0 meshes were computationally time consuming.

Example 4. The frames of the previous examples contained slender members where the transverse shear deformation is negligible. The shear deformable C^0 meshes are adopted here to study the dynamic behaviour of deeper beams with predominant transverse shear strain.

A simply supported beam analysed by Bathe *et al.* [19] and later on by Liu and Lin [20] is considered here for studying the efficiency of C^1 and C^0 meshes. The length to depth ratio of the beam is 15 and is subjected to a uniformly distributed load of $0.75p_0$, where p_0 is the static collapse load and perfectly plastic model with a yield stress of 0.5E05 psi is adopted as shown in Fig. 13.

The beam has been discretized by six C^1 elements and four trilinear meshes. The elastic and elastoplastic response histories are plotted in Fig. 14. Bathe *et al.* had made use of a eight-noded plane stress

Table 5. Comparison of computational costs of C^1 and C^0 meshes (example 3)

Mesh type	(Δt) adopted (sec)	Range of integration (sec)	Number of steps	CPU time (sec)
C^1	0.1E − 2	3.0	3E3	70
Linear	0.1E − 3	3.0	3E4	628
Bilinear	0.5E − 4	3.0	6E4	2509
Trilinear	0.5E − 4	3.0	6E4	3711

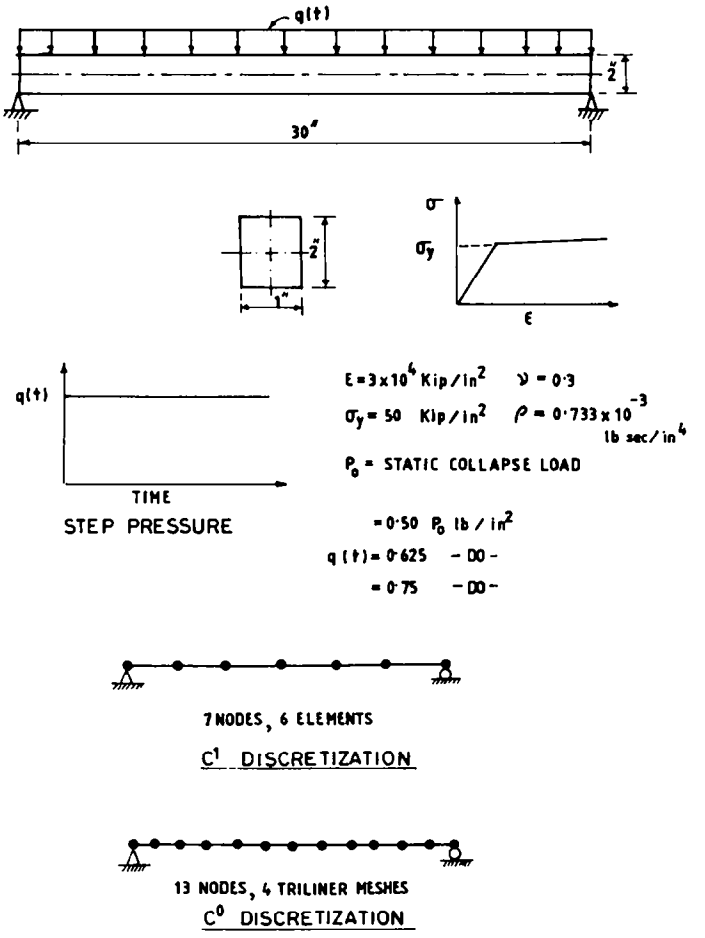

Fig. 13. A simply supported beam with suddenly applied uniformly distributed load [19].

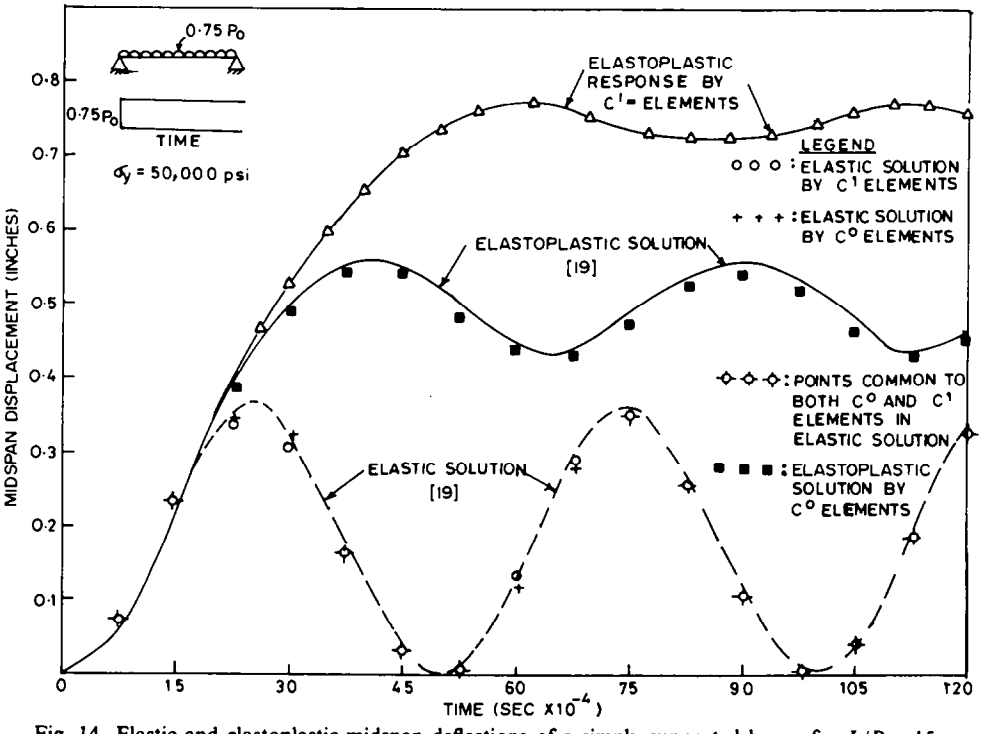

Fig. 14. Elastic and elastoplastic midspan deflections of a simply supported beam, for $L/D = 15$.

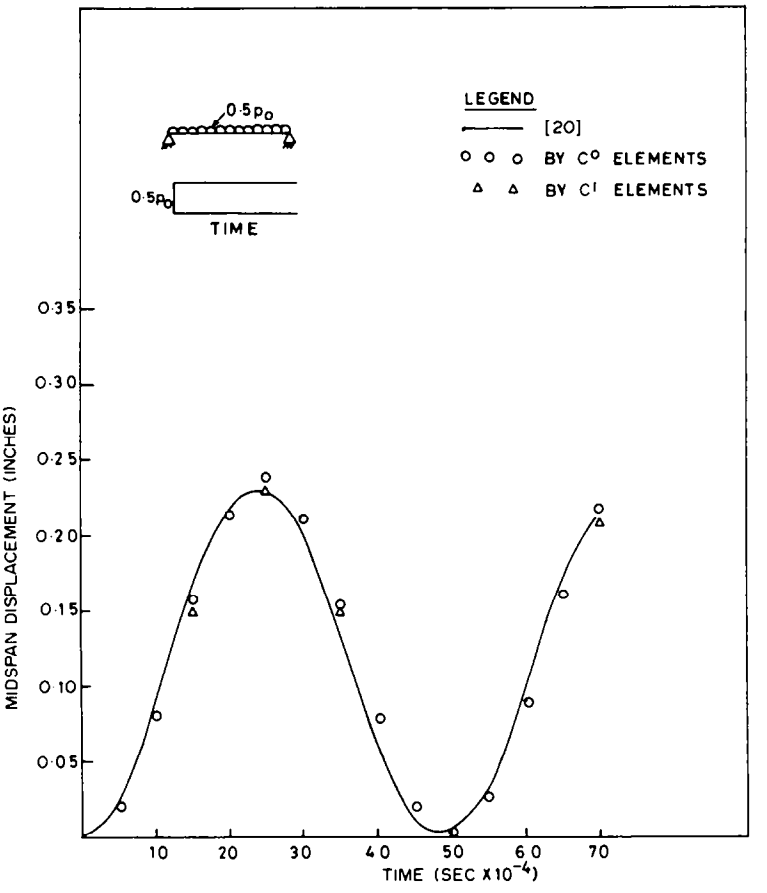

Fig. 15. Elastic midspan displacements of a simply supported beam for $L/D = 15$.

two-dimensional element and von Mises yield criterion to analyse the beam. It can be observed that though both C^1 and C^0 elements yield results closer to that of Bathe *et al.*'s for elastic conditions, for elastoplastic conditions C^1 predictions have higher peaks and periods, while C^0 is very close to that of Bathe *et al.*'s.

For another loading of $0.5p_0$, the elastic displacement history is given in Fig. 15. Here both C^0 and C^1 elements agree very closely with the reference values. For the same loading, but for elastoplastic analysis, as shown in Fig. 16, the deviation of C^1 results is quite high in comparison with C^0 output, which is very close that of Liu and Lin.

For yet another loading of $0.625p_0$, the variation of C^1 results in the elastoplastic analysis with respect to C^0 and the reference results is shown in Fig. 17.

The strain hardening has been incorporated in the material model for the same loading, and the response history is plotted in Fig. 18. For the value of β equal to 0.25, the deviation of C^1 predictions are more compared to the reference output or C^0 results.

Example 5. Another simply supported beam with a suddenly applied concentrated load at the centre of its span is discretized with four trilinear meshes and six C^1 elements. Making use of the symmetry of the geometry and loading, one fourth of the same beam is also analysed as a plane stress problem by using six numbers of eight-noded serendipity element, for comparing the results of both C^0 and C^1 elements.

The details of the beam and loading are shown in Fig. 17. The transient response of the beam, for different L/D ratios are plotted in Figs 20–24.

It can be observed that for slenderness ratio less than or equal to two, neither C^0 nor C^1 element predicts the response closer to that of serendipity element.

When L/D ratio lies in the range of three to eight, trilinear mesh yields results very closer to the two-dimensional elements than the C^1 elements. As shear deformation would be predominant, in this region of L/D ratio, C^0 elements perform better (as this deformation has been taken into account in the formulation) than C^1 elements.

As the aspect ratio reaches the value of nine and above, both the elements can be seen to yield results closer to those obtained from the plane stress solution.

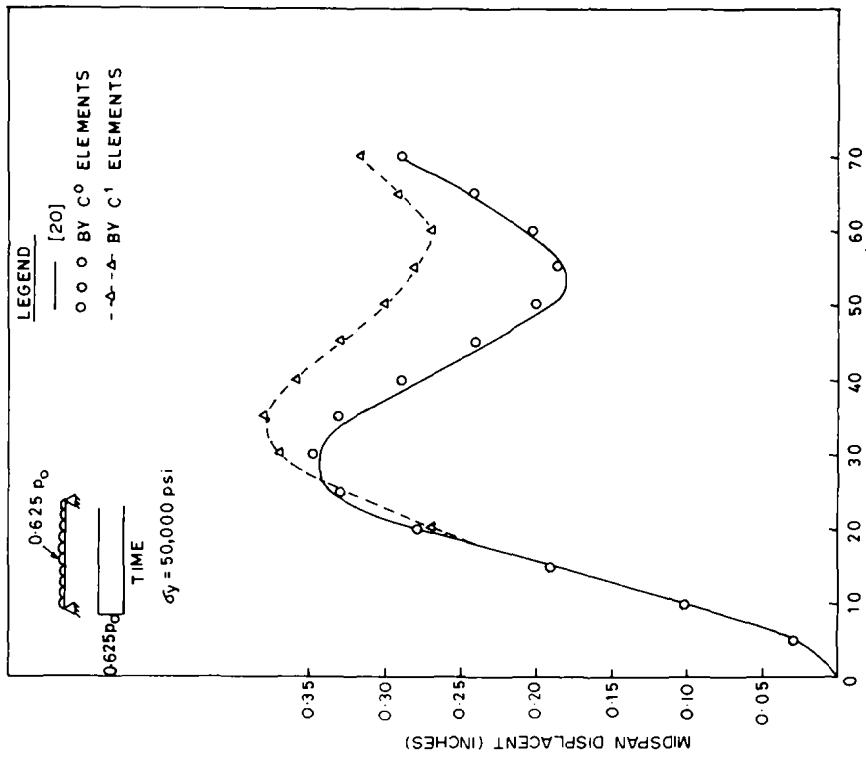

Fig. 17. Elastoplastic midspan displacements of a simply supported beam for $L/D = 15$.

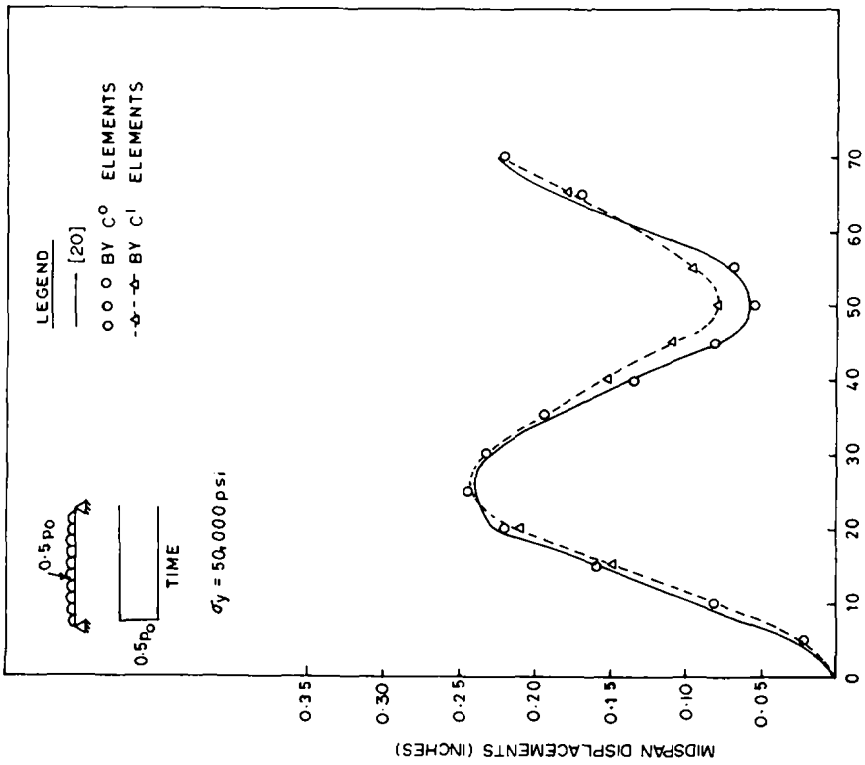

Fig. 16. Elastoplastic midspan displacements of a simply supported beam for $L/D = 15$.

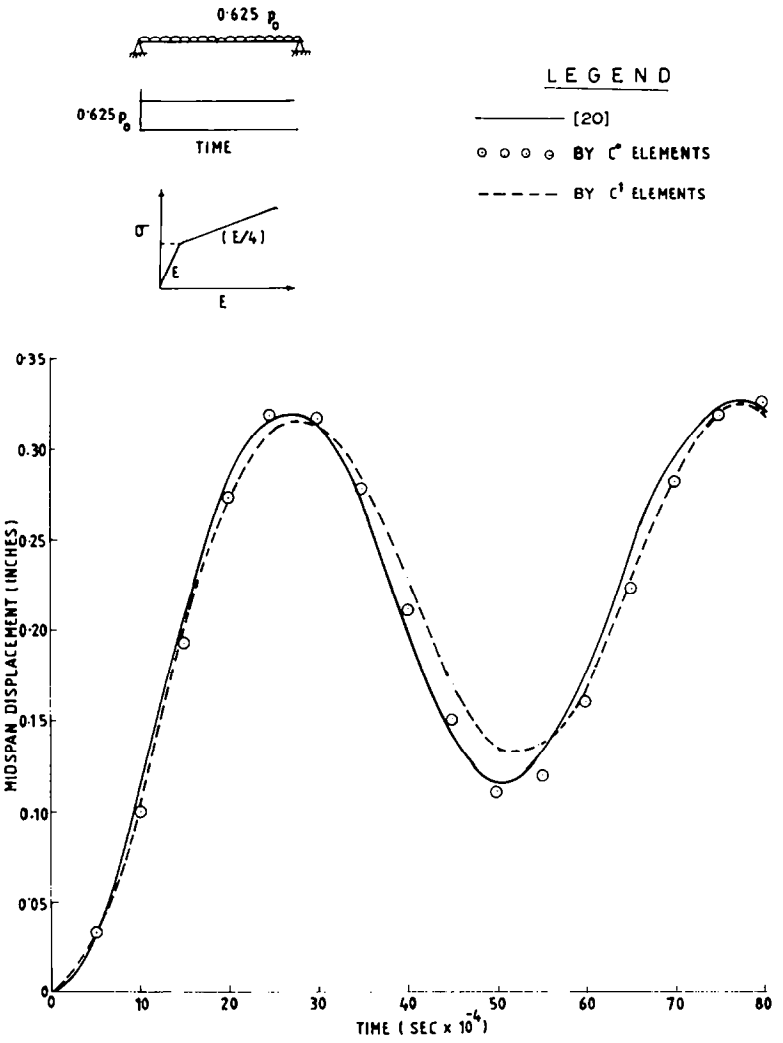

Fig. 18. Elastoplastic midspan displacements of a simply supported beam with strain hardening effect for $L/D = 15$.

6. CONCLUSIONS

Based on the results from the numerical analysis in the preceding sections, the following conclusions have been arrived at:

1. Three, C^0 two-noded linear elements, denoted as trilinear mesh can be considered computationally equivalent to a C^1 element.

2. The bilinear and linear C^0 meshes always yield stiffer results compared to the trilinear mesh, thus rendering themselves practically not so much useful as the trilinear one.

3. For any frame member with slenderness ratio more than 15, both the C^1 elements and C^0 trilinear mesh would yield accurate results in both elastic and inelastic conditions.

4. When the aspect ratio is between 9–15, the C^1 elements would correctly predict the response of frames, only if they are elastic. When the material displays elastoplastic behaviour, C^1 elements fail to yield the correct response, in this range of slenderness ratio. But the trilinear mesh, on the contrary, gives precisely, the time history of frames, both in elastic and inelastic conditions.

5. In the case of deep members with L/D ratios between 3–8, C^0 mesh predicts the response much closer to the reality and better than C^1 elements, thus rendering the latter ones unsuitable for the analysis of such members.

6. When the ratio of length to depth falls below two, both the elements fail to predict the response.

7. The only factor weighing against the C^0 mesh is its high computational cost. In this aspect, C^1 elements score better than their counterparts.

8. Though the C^0 elements are expensive, they are indeed indispensable for the transient analysis of deep beams/frames, particularly, in the nonlinear range.

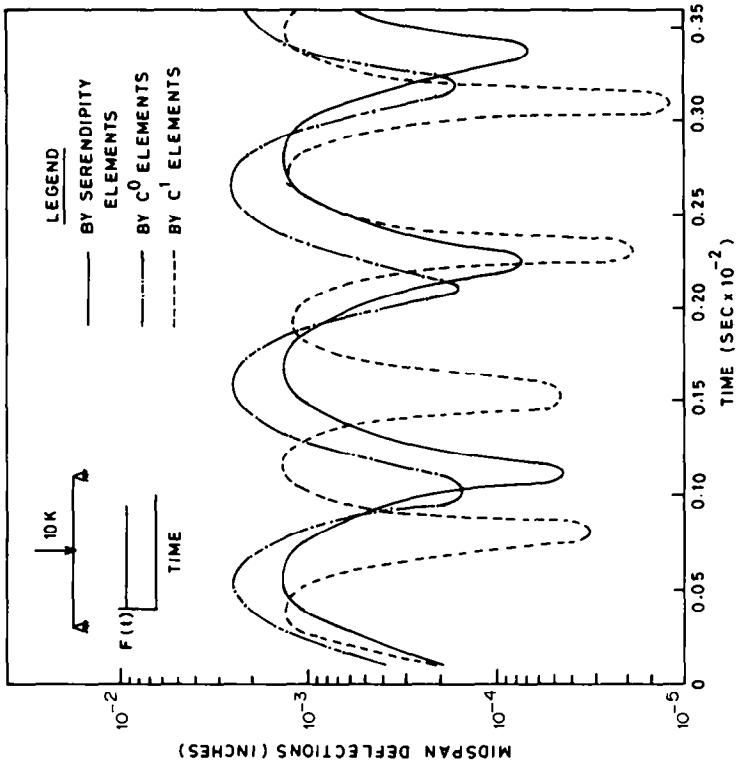

Fig. 20. Comparison of the solutions of a simply supported beam, using C^0 and C^1 elements for $L/D = 2$.

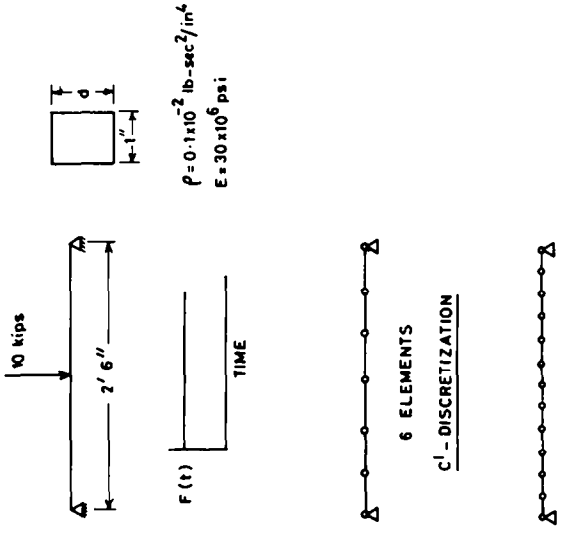

Fig. 19. A simply supported beam with a suddenly applied midspan load.

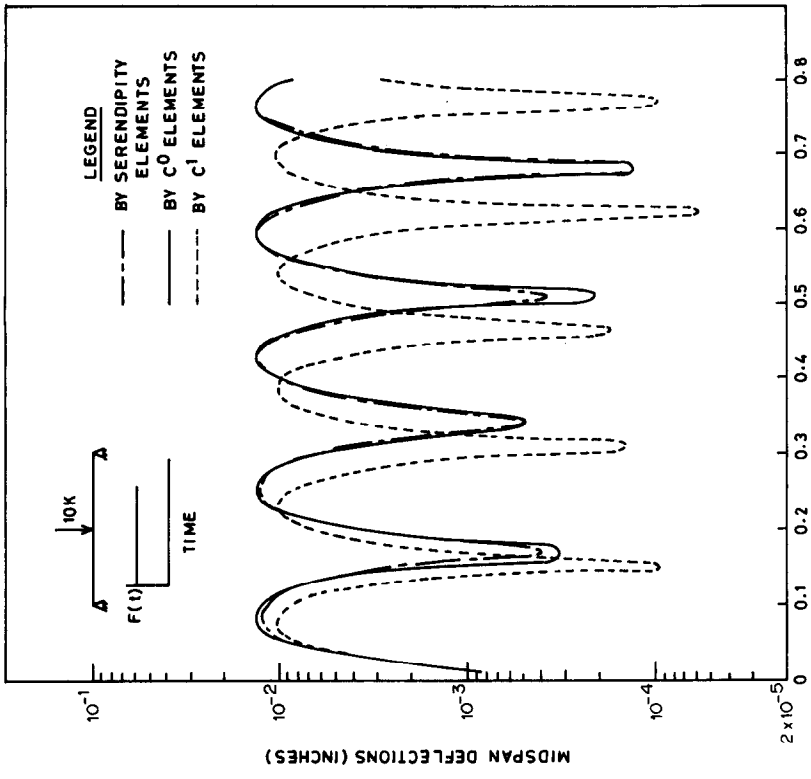

Fig. 22. Comparison of the solutions of a simply supported beam, using C^0 and C^1 elements for $L/D = 4$.

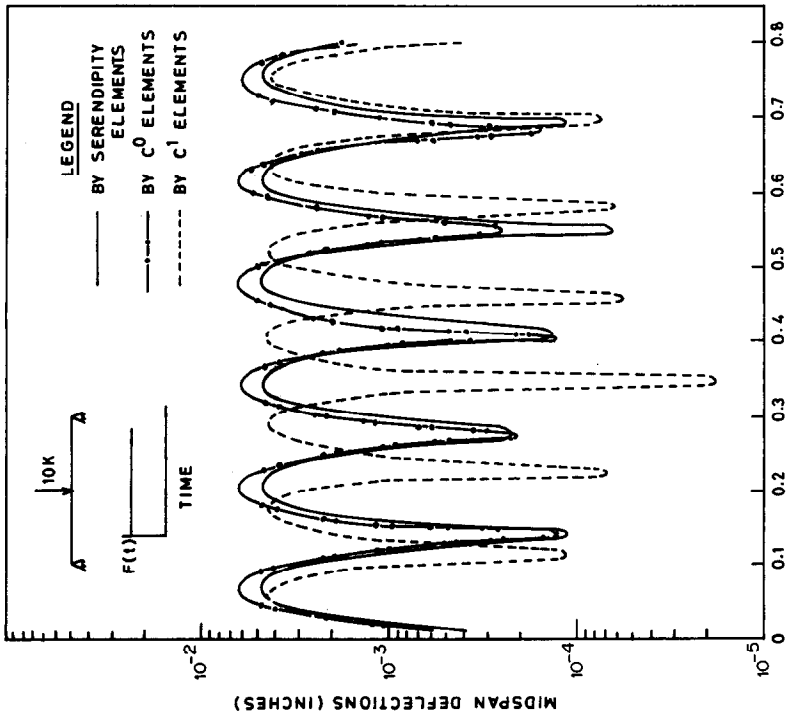

Fig. 21. Comparison of the solutions of a simply supported beam, using C^0 and C^1 elements for $L/D = 3$.

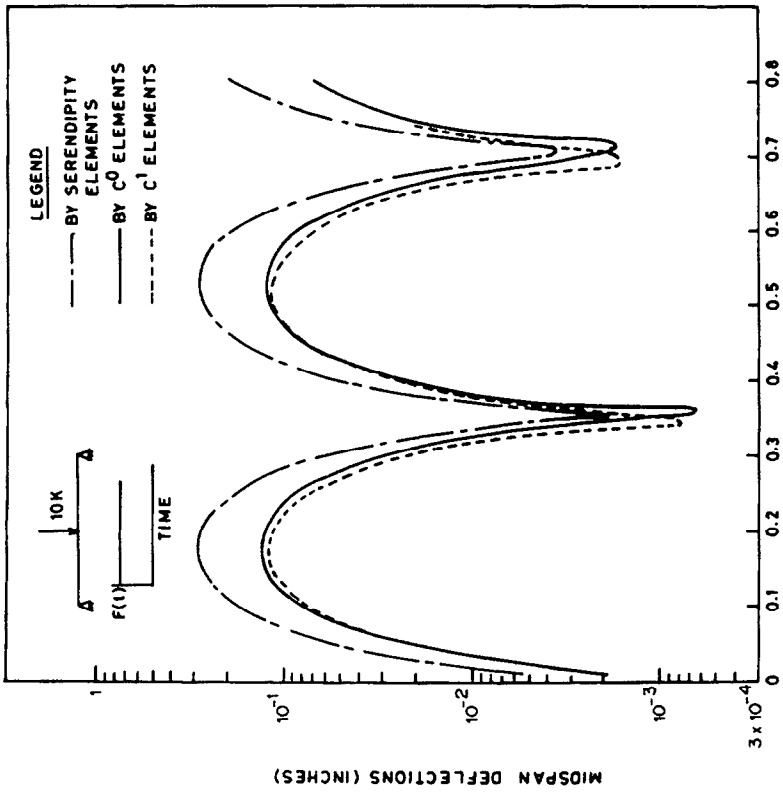

Fig. 24. Comparison of the solutions of a simply supported beam, using C^0 and C^1 elements for $L/D = 9$.

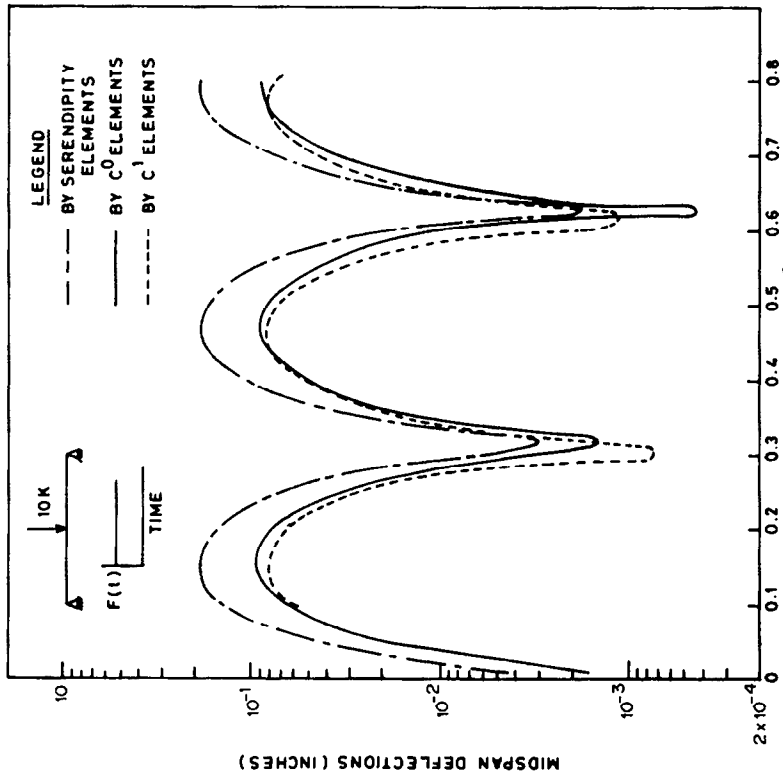

Fig. 23. Comparison of the solutions of a simply supported beam, using C^0 and C^1 elements for $L/D = 8$.

REFERENCES

1. T. G. Toridis and K. Khozeimeh, Inelastic response of frames to dynamic loads. *J. Struct. Div., ASCE* **97,** 847–863 (1971).
2. R. W. H. Wu and E. A. Witmer, Finite-element analysis of large elastic–plastic transient deformations of simple structures. *AIAA Jl* **9,** 1719–1724 (1971).
3. T. Y. Kam and S. C. Lin, Nonlinear dynamic analysis of inelastic steel plane frames. *Comput. Struct.* **28,** 535–542 (1988).
4. S. P. Timoshenko, On the correction for shear in differential equations for transverse vibrations of prismatic bars. *Phil. Mag.* **41,** 744–746 (1921).
5. T. J. R. Hughes, R. L. Taylor and S. Kanoknukulchai, A simple and efficient finite element for bending. *Int. J. Numer. Meth. Engng* **11,** 1529–1543 (1977).
6. M. Mukhopadhyay and D. K. Dinker, Isoparametric linear bending element and one point integration. *Comput. Struct.* **9,** 365–369 (1978).
7. T. Kant and P. B. Kulkarni, A C^0 continuous linear beam/bilinear plate flexure element. *Comput. Struct.* **22,** 413–425 (1986).
8. I. M. Kani and R. E. McConnel, A simple and efficient beam element for the combined nonlinear analysis of frameworks. *Comput. Struct.* **25,** 457–462 (1987).
9. S. R. Marur and T. Kant, Modified form of central difference predictor scheme for damped nonlinear systems, to be published.
10. O. C. Zienkiewicz, *The Finite Element Method*, 3rd edn. McGraw-Hill, London (1979).
11. S. R. Marur and T. Kant, A stress correction procedure for the analysis of inelastic frames under transient dynamic loads, to be published.
12. D. R. J. Owen and E. Hinton, *Finite Elements in Plasticity: Theory and Practice*. Pineridge Press, Swansea (1980).
13. J. W. Leech, P. T. Hsu and E. W. Mack, Stability of a finite difference method for solving matrix equations. *AIAA Jl* **3,** 2173–2174 (1965).
14. B. M. Irons and S. Ahmad, *Techniques of Finite Elements*. Ellis Horwood, Chichester (1980).
15. T. Belytschko, Explicit time integration of structure–mechanical systems. In *Advanced Structural Dynamics* (Edited by J. Donea). Applied Science, London (1980).
16. E. Hinton, T. Rock and O. C. Zienkiewicz, A note on mass lumping and related processes in the finite element method. *Int. J. Earthquake Engng Struct. Dyn.* **4,** 245–249 (1976).
17. J. M. Biggs, *Introduction to Structural Dynamics*. McGraw-Hill, New York (1964).
18. S. I. Hilmy and J. F. Abel, Material and geometric nonlinear dynamic analysis of steel frames using computer graphics. *Comput. Struct.* **21,** 825–840(1985).
19. K. J. Bathe, H. Ozdemir and E. L. Wilson, Static and dynamic geometric and material nonlinear analysis. Report No. UCSESM 74-4, University of California, Berkeley (1974).
20. S. C. Liu and T. H. Lin, Elasto-plastic analysis of structures using known elastic solutions. *Int. J. Earthquake Engng Struct. Dyn.* **7,** 147–160 (1979).